

MRS Advances © 2016 Materials Research Society DOI: 10.1557/adv.2016.434

Synthesis and Characterization of Empty Silicon Clathrates for Anode Applications in Li-ion Batteries

Kwai S. Chan¹, Michael A. Miller¹, Carol Ellis-Terrell¹, and Candace K. Chan²

ABSTRACT

Several processing methods were developed and evaluated for synthesizing empty silicon clathrates. A solution synthesis method based on the Hofmann-elimination oxidation reaction was successfully utilized to produce 20 mg of empty Si $_{46}$. Half-cells using the Si $_{46}$ electrodes were successfully cycled for 1000 cycles at rate of 5.3C. The capacity of the Si $_{46}$ electrode in long-term tests was 675 mAh/g at the 4^{th} cycle, but increased to 809 mAh/g at 50 cycles. The corresponding Coulombic efficiency was better than 99%. The capacity dropped from 809 to 553 mAh/g after 1000 cycles while maintaining a 99% Coulombic efficiency. In comparison, a Ba $_8$ Al $_8$ Si $_{38}$ electrode could be cycled for about 200 cycles with a lower capacity and Coulombic efficiency. Potential applications of empty silicon clathrates as anode materials in Li-ion batteries are discussed.

INTRODUCTION

Low-cost advanced anode materials with high-energy density, high-power density, and longer cycle life are needed for plug-in hybrid (PHEV) and electric vehicle (EV) applications. In an effort to address these needs, we explored the viability of silicon clathrates (Type I) as an anode material for potential applications in lithium (Li)-ion batteries for PHEV and EV. This project, funded by Department of Energy (DOE), focused on the development of scalable synthesis, complete characterization of electrochemical performance, and the design and fabrication of prototype anodes for evaluation.

Silicon clathrate, an allotrope of silicon, is composed of sp³ bonded silicon atoms arranged in cage-structures. It consists of crystalline Si with a regular arrangement of 20- and 24-atom cages fused together through five atom pentagonal rings (Type I clathrate). It has a simple cubic structure with a lattice parameter of 10.335 Å and 46 Si atoms per unit cell (Si₄₆). The crystal structure (Space Group $Pm\overline{3}n$) of the Si₄₆ clathrate is different from the common form of crystalline Si (c-Si), which is diamond cubic (Space Group $Fd\overline{3}m$) with a lattice parameter of about 5.456 Å.

First-principles computations [1, 2] revealed that significant amounts of Li ions can be inserted into and extracted from the cage structure of silicon clathrates without substantial volume changes or pulverization of the cage structure. Theoretical predictions of the total, occupiable, and accessible volumes within Type I silicon clathrate structures indicate that the empty spaces within the cage structures are accessible to Li and amenable to Li intercalation

¹ Southwest Research Institute[®], 6220 Culebra Road, San Antonio, TX 78238-5166, U.S.A.

² Arizona State University, 501 E. Tyler Mall, ECG 301, Tempe, AZ 85287-8706, U.S.A.

through electrochemical means, while overcoming the usual problems of irreversible volume expansion encountered in diamond cubic and/or amorphous Si-based anodes. The calculations showed that as high as 48 Li atoms can be inserted into an empty Si₄₆ cage structure without causing a significant volume expansion (less than 8%) [1]. On this basis, silicon clathrates are attractive as anode materials for Li-ion battery applications, as demonstrated in a recent study on anodes made from framework substituted Type I clathrate compounds of Ba₈Al_ySi_{46-y} form [3].

The objective of this article is to highlight results from the synthesis of empty silicon clathrates, the fabrication of Si clathrate anodes for half-cell electrochemical characterization, and the long-term cycleability and performance of empty silicon clathrate anodes. For the purpose of illustrating the effect of a guest atom in the cage structure, the long-term performance of empty Si clathrate anodes is compared to those of $Ba_8Al_8Si_{38}$. This paper also reports on the results of applying several ex-situ techniques to interrogate the structural and mechanical state of Si clathrate anodes as a function of lithiation/delithiation cycles for Type I $Ba_8Al_8Si_{38}$.

EXPERIMENTAL

Several different processing routes were employed to synthesize silicon clathrates appropriate for use as anode materials [1]. These methods included: (1) high-pressure, high-temperature Walker-type multi-anvil techniques [1], (2) vacuum arc-melting synthesis [1], (3) direct synthesis of guest-free Si clathrate by plasma-enhanced magnetron sputtering (PEMS) of Si into an ionic liquid in vacuum [1], and (4) batch synthesis via soft oxidation of Na₄Si₄ [1,4]. The vacuum arc-melting method was successful in synthesizing Ba-stabilized, Al-substituted Si clathrates in moderate quantities (200 g) while the fourth method was successful in synthesizing empty (guest-free) Si clathrates (20 mg), but with relatively low yields. Soft oxidation of Na₄Si₄ is emphasized in this paper since this method produced sufficient amounts of empty Si clathrates for fabrication of electrodes for half-cell cyclic testing.

In batch synthesis via soft oxidation of Na_4Si_4 , process methods were devised to enable the conversion of fuel-grade sodium silicide ($NaSi_{1.5}$) to yield the highest purity of the Zintl phase Na_4Si_4 possible by varying excess additions of NaH combined with the silicide. XRD analyses of the thermal transformation products confirmed the conversion of $NaSi_{1.5}$ to the Zintl phase Na_4Si_4 , when 10% excess NaH was combined with the silicide during thermal processing. Higher additions of NaH did not manifest the required XRD reflections for the Zintl phase. Using these process conditions, about 10 g of Na_4Si_4 was synthesized for subsequent use in the batch synthesis of Si_{46} .

After successful conversion of Na_4Si_4 , this Zintl compound was combined with an alkylammonium-AlCl $_3$ ionic liquid (IL) to synthesize empty silicon clathrate (Si_{46}) via Hofmann-type elimination-oxidation reaction scheme done in solution [4]. The XRD analysis (Figure 1) of the reaction product indicated that the desired Type I clathrate was formed along with unreacted Zintl compound and the reaction by-products. The product (~20 mg) was purified further for subsequent electrochemical measurements as an anode material, but some reaction by-products still remained as suggested by the extra peaks in the XRD pattern shown in Figure 1.

Several different additive and binder combinations were investigated in the fabrication of silicon clathrate anodes using $Ba_8Al_8Si_{38}$. The framework-substituted Type I clathrate, ($Ba_8Al_8Si_{38}$), synthesized in bulk (200 g) by vacuum arc-melting, was processed via ball milling and sequential particle separation to produce sub-micron particles, as shown in Figure 2. The milled product was combined with a conductive additive to make a slurry. The conductive

additive used included (1) 0.2 to 4 wt.% Graphenol®, (2) 10 wt.% Super P carbon, (3) 20 wt.% Super P carbon, and (4) 25 wt.% Super P carbon. The resulting slurries were then used to cast thin-film anodes for electrochemical half-cell evaluation. Based on the half-cell performance, Super P carbon was selected at a loading of 25 wt.% for long-term half-cell cyclic testing.

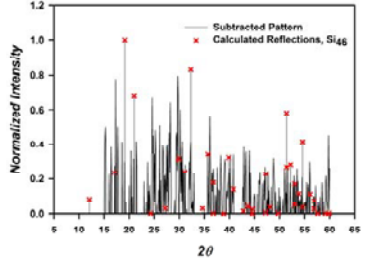


Figure 1. Overlay of powder XRD patterns for the synthesized product and the calculated reflections of empty clathrate (Si₄₆), after subtraction of impurity phases.

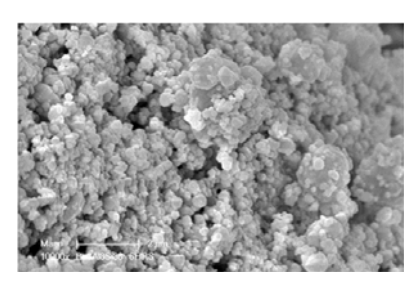


Figure 2. Particle morphology of processed Ba₈Al₈Si₃₈ milled powder for prototype anode.

Guest-free (empty) Si_{46} clathrates synthesized by soft oxidation of Na_4Si_4 were combined with a conductive additive (25 wt.% Super P) to make a slurry. The resulting slurries were then used to cast thin-film anodes for electrochemical half-cell evaluation.

The long-term cyclic performance of a half-cell of $Ba_8Al_8Si_{38}$ and a half-cell of guest-free Si_{46} were evaluated using a three-electrode split cell with a polypropylene (PP) separator film. The framework-substituted clathrate electrode consisted of $Ba_8Al_8Si_{38}$ with 25% Super P and 20% PVDF by weight. The active area of the electrode was 1.766 cm² with a thickness of 165 μ m. The mass of the active material was 1.216 mg. The empty silicon clathrate electrode consisted of Si_{46} with 25% Super P and 20% PVDF by weight. The active area of the electrode was also 1.766 cm² with a thickness of 89.2 μ m. The mass of the active material was 0.3485 mg. The electrolyte was 1 M LiPF₆ in EC/DEC/FEC in 45:45:10 volume ratios.

RESULTS

Figure 3(a) shows the capacity (left scale) and the Coulombic efficiency (right scale) as a function of cycle number for the Ba₈Al₈Si₃₈ electrode from 4 to 50 cycles. The first three cycles, which were in the SEI formation phase, are not presented in this figure. As shown in Figure 3(a), the capacity of the Ba₈Al₈Si₃₈ anode was 214 mAh/g at 4th cycle, but dropped to 74 mAh/g at 50 cycles at 2.8C. The corresponding Coulombic efficiency was 98.5%. Upon further cycling, the capacity dropped to 25 mAh/g after 1000 cycles, as shown in Figure 3(b).

Figure 4(a) shows the capacity (left scale) and the Coulombic efficiency (right scale) as a function of cycle number of the Si₄₆ anode from 4 to 50 cycles. The first three cycles, which were in the SEI formation phase, are again not presented in this figure. As shown in Figure 4(a), the capacity of the Si₄₆ anode was 675 mAh/g at 4th cycle, but increased to 809 mAh/g at 50 cycles at 5.3C. The corresponding Coulombic efficiency was 99%. After a temporary stop at the 50th cycle, the capacity jumped to 1030 mAh/g at the 51st cycle as shown in Figure 4(b).

Upon further cycling, the capacity dropped from 1030 to 553 mAh/g after 1000 cycles, as shown in Figure 4(b).

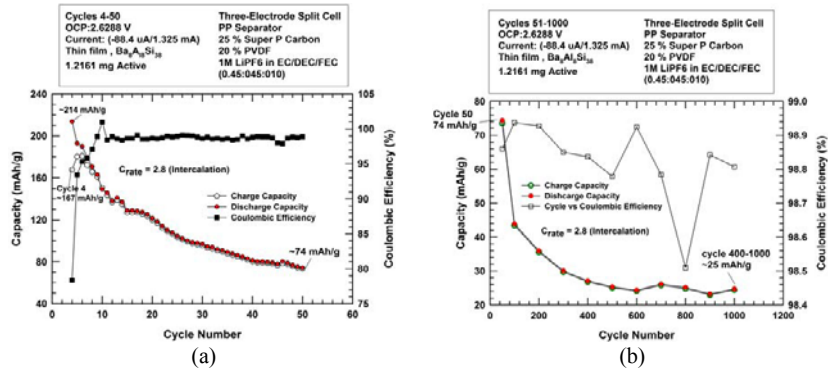


Figure 3. Capacity and Coulombic efficiency of a Ba₈Al₈Si₃₈ electrode during cycling (a) from the 4^{th} to the 50^{th} cycle, and (b) from the 51^{st} to the 1000^{th} cycle.

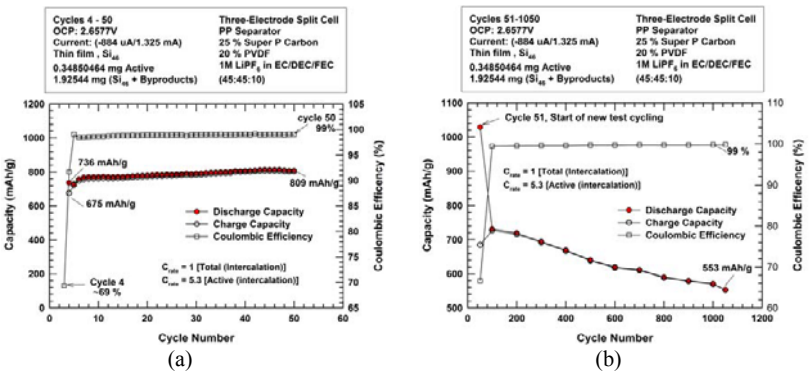


Figure 4. Capacity and Coulombic efficiency of a Si₄₆ electrode during cycling (a) from the 4th to the 50th cycle, and (b) from the 51st to the 1000th cycle.

DISCUSSION

Two *ex-situ* techniques were employed to map the structural and mechanical state of the clathrate electrodes before and after lithiation. In particular, structural and compositional analyses of Ba₈Al₈Si₃₈ were performed using high-resolution magic angle spinning nuclear magnetic resonance (MAS-NMR), and neutron diffraction measurements (facilitated through Oak Ridge National Laboratory)

In the case of NMR, the chemical shift environments of ²⁹Si and ²⁷Al along with that of the ⁷Li were probed to study the effects of lithium intercalation on structural parameters and local

interactions. Notably, the 27 Al-NMR spectra acquired for the unlithiated and lithiated clathrate, shown in Figure 5, show three distinct magnetic environments, most likely associated with the three known framework substitution sites in the dodecahedron and tetrakaidecahedron cages of the Type I clathrate structure. Upon lithiation, only the 16i framework sites near 80 ppm appear to be affected by the presence of Li^+ , but only with respect to relative amplitude when comparing the integration ratios for the three lines. No significant change in chemical shift was observed, suggesting that Li^+ interactions with Al framework atoms are weak and the structural order of the framework remains intact. Only the spin-lattice (T_1) relaxation times are influenced by the local structuring of Li^+ near the 16i framework sites giving rise to a change in relative amplitude after lithiation. Additionally, the near-baseline resolution of the NMR lines corresponding to the three framework sites is remarkable from the viewpoint of substitutional order. This result indicates that Al substitution of framework atoms during synthesis does not occur randomly, but rather prefers ordered substitution for the bulk material. By contrast, random substitution would otherwise result in one broad peak due to the superposition of all site-substitution combinations.

Neutron diffraction measurements (Figure 6) were used to study the crystal structure of Ba₈Al₈Si₃₈ after lithiation. Figure 6 shows that the neutron diffraction patterns for the unlithiated (blue) and lithiated Ba₈Al₈Si₃₈ anodes exhibit the same intact structure and lattice constant, suggesting that the crystalline structure of the clathrate is unaffected during lithiation.

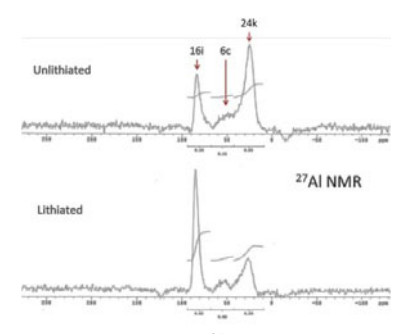


Figure 5. Solid-state ²⁷Al NMR spectra acquired for unlithiated ($Ba_8Al_8Si_{38}$) and lithiated ($Li_xBa_8Al_8Si_{38}$) clathrate anode material. The results show near-baseline resolution of the three known and magnetically-distinct framework substitution sites for a Type I structure: 6c, 16i, and 24k.

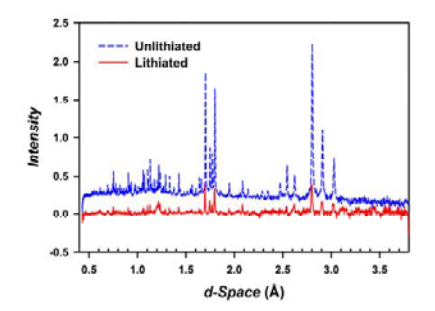


Figure 6. Neutron diffraction patterns obtained for Ba₈Al₈Si₃₈ before (top) and after lithiation (bottom), providing evidence that the clathrate framework remains structurally intact up to its theoretical capacity.

The long-term cyclic tests suggest that Li atoms can be inserted and extracted from the cage cavities of both $Ba_8Al_8Si_{38}$ and Si_{46} clathrates. The presence of Ba guest atoms inside the Al_8Si_{38} framework may have hindered the insertion and extraction of Li atoms from the cage structure and limits cycleability. In contrast, the insertion and removal of Li atoms from the cage cavities of empty Si_{46} is comparatively easier and therefore leads to improved Coulombic efficiency, higher capacity, and longer life compared to $Ba_8Al_8Si_{38}$. The observed capacities of empty Si_{46} were 675 to 809 mAh/g during stable cycling. The number of Li atoms required to achieve these

observed capacities are computed to be 39 to 49, which are in agreement with theoretical predictions of a maximum of \approx 48 Li based on density functional theory [1]. At these levels of capacities, Li atoms can be inserted and extracted with small volume changes (\approx 40%). At the peak capacity (1030 mAh/g), the number of Li atoms inserted was computed to be 66 at which point the lithiated Si₄₆ cage structure began to expand substantially [1]. The overlithiation, lattice expansion, and possible damage to the cage structure may have been responsible for the lower capacities after the 51st cycle.

CONCLUSIONS

Several processing methods have been developed and evaluated for synthesizing Bastabilized and empty silicon clathrates. An industrial vacuum arc-melting method is a viable means for synthesizing Ba-stabilized Al-substituted silicon clathrates (Ba₈Al₈Si₃₈) in moderate quantities (~200 g). A solution synthesis method based on the Hofmann-elimination oxidation reaction was successfully utilized to produce about 20 mg of empty Si₄₆.

Half-cells with $Ba_8A_1 RSi_{38}$ and Si_{46} electrodes were successfully cycled for up to 1000 cycles in the long-term cyclic durability tests. The capacity of the $Ba_8A_1 RSi_{38}$ anode was 214 mAh/g at 4^{th} cycle, but dropped to 74 mAh/g at 50 cycles at 2.8C. The corresponding Coulombic efficiency was 98.5%. Upon further cycling, the capacity dropped to 25 mAh/g after 1000 cycles. The capacity of the Si_{46} electrode in long-term test was 675 mAh/g at 4^{th} cycle, then increased to 809 mAh/g at 50 cycles at 5.3C. The corresponding Coulombic efficiency was greater than 99%. The capacity dropped from 809 to 553 mAh/g after 1000 cycles while maintaining a 99% Coulombic efficiency. These results demonstrate that empty Si_{46} electrodes exhibit long-term cyclic durability in excess of 1000 cycles and may be considered as potential anode materials for Li-ion batteries.

ACKNOWLEDGMENTS

This work was supported by the Batteries for Advanced Transportation Technologies (BATT) Program at Lawrence Berkeley National Laboratory (LBNL) through Contract No. DEAC0205CH11231, with Dr. Michel Foure at LBNL as program manager. The contribution of C.K.C. was supported by the National Science Foundation through Grant No. DMR-1206795 and Fulton School of Engineering, Arizona State University.

REFERENCES

- K. S. Chan and M. A. Miller, Anodes—Synthesis and Characterization of Silicon Clathrates for Anode Applications in Lithium-Ion Batteries, *Energy Storage R&D*, FY2014 Final Report, Southwest Research Institute, 2014.
- X. Peng, Q. Wei, Y. Li, and C. K. Chan, J. Phys. Chem. C, 119, 28247-28257 (2016).
- Y. Li, R. Raghavan, N. A. Wagner, S. K. Davidowksi, L. Baggetto, R. Zhao, Q. Cheng, J. L. Yarger, G. M. Veith, C. Ellis-Terrell, M. A. Miller, K. S. Chan, and C. K. Chan, *Advanced Science*, 2015, 1500057. DOI: 10.1002/advs.201500057
- A. M. Guloy, R. Ramlau, Z. Tang, W. Schnelle, M. Baitinger, and Y. Grin, *Nature*, 443, 320-323 (2006). DOI: 10.1038/nature05145